www.czasopisma.pan.pl PAN POLSKA AKADEMIA NAUK www.journals.pan.pl

A R C H I V E S O F M E T A L L U R G Y A N D M A T E R I A L S

Volume 56 2011 Issue 4

DOI: 10.2478/v10172-011-0105-x

T. KURŞUN*

EFFECT OF THE GMAW AND THE GMAW-P WELDING PROCESSES ON MICROSTRUCTURE, HARDNESS, TENSILE AND IMPACT STRENGTH OF AISI 1030 STEEL JOINTS FABRICATED BY ASP316L AUSTENITIC STAINLESS STEEL FILLER METAL

TWARDOŚĆ, WYTRZYMAŁOŚĆ NA ROZCIĄGANIE I UDARNOŚĆ ZŁĄCZY ZE STALI AISI 1030 WYKONANYCH Z UŻYCIEM SPOIWA Z AUSTENITYCZNEJ STALI NIERDZEWNEJ ASP316L

In this study, medium-carbon steel (AISI 1030) plates of 10 mm thickness, were welded by using the synergic controlled pulsed (GMAW-P) and manual gas metal arc (GMAW) welding techniques. Constant wire feed speed, voltage, welding speed and gas flow rates (3.2 m/min, 22.5 V, 4 mm/s, 16 l/min) and ASP316L austenitic stainless steel filler metal were used in these techniques. The interface appearances of the welded samples were examined by optical microscopy (OM), scanning electron microscopy (SEM), energy dispersive spectrometry (EDS) and X-Ray diffraction (X-RD). In order to determine mechanical properties of samples, the tensile, impact and microhardness tests were conducted. The GMAW-P joints of AISI 1030 steel couples showed superior tensile strength, less grain growth and narrower heat affected zone (HAZ) when compared with GMAW joints, and this was mainly due to lower heat input, fine fusion zone grain and higher fusion hardness.

Keywords: welding, mechanical properties, GMAW-P

W pracy, płyty ze średniowęlowej stali (AISI 1030) o grubości 10 mm były spawane technikami impulsowego (GMAW-P) i ręcznego spawania w gazie (GMAW). W obu technikach wykorzystano stałą prędkość podawania drutu, napięcie, szybkość spawania i wielkość przepływu gazu (odpowiednio: 3.2 m/min, 22.5 V, 4 mm/s, 16 l/min), oraz austenityczną stal nierdzewną ASP316L jako spoiwo. Otrzymane próbki spoin badane były za pomocą mikroskopii optycznej, skaningowej mikroskopii elektronowej i mikroanalizy rentgenowskiej, oraz dyfrakcji rentgenowskiej. W celu określenia właściwości mechanicznych próbek wykonano próby rozciągania, udarności i mikrotwardości. Złącza otrzymane techniką spawania impulsowego charakteryzują się wyższą wytrzymałością na rozciąganie, mniejszym wzrostem ziarna i węższą strefą wpływu ciepła w porównaniu do złączy otrzymanych techniką spawania ręcznego. Jest to spowodowane głównie mniejszą ilością ciepła, drobnym ziarnem w przetopionej strefie i jej większą twardością.

1. Introduction

AISI 1030 steel contains about 0.30 % carbon and a relatively low percentage of manganese has limited weldability. Medium-carbon steels are used extensively in machinery and tools. Often these steels are selected for their wear resistance rather than high strength, and their parts frequently must be heat treated to meet in-service strength requirements [1].

Fusion welding is an ideal and economical means of achieving good productivity. Fusion welding through GMAW is achieved by coalescence of metals by melting continuously feed current-carrying wire. Its wide popularity is due to practical advantages offered like: continuously feed electrode, flux free operation, relatively low operator skills required, ease of automation. GMAW can weld wide range of metals and welding in any positions possible. GMAW is also widely used by the sheet metal industry, due to its high efficiency and suitability in automated processes. GMAW is used on all thicknesses of steels, aluminum, nickel, stainless steels etc. The GMAW is suitable both for steel and unalloyed, low-alloy and high-alloy based materials. On the other hand, the process of GMAW is used for welding aluminum and copper materials. But the quality of weld obtained from GMAW depends on various welding parameters like voltage, current etc. Various welding parameters influence transfer mode in GMAW that influences weld quality. Hence, in a welding system, principal sources of disturbances are welding parameters, which need constant control and adjustment to achieve best quality. At relatively low currents, GMAW operates in

* CUMHURIYET UNIVERSITY, FACULTY OF TECHNOLOGY, SIVAS, TURKEY

the globular metal transfer mode. It is characterized by periodic formation of big droplets at the end of electrodes, which detach due to gravitational force into the weld pool. This metal transfer mode suffers from lack of control over molten droplets and arc instability due to formation of big droplets. At higher currents, the process transits to spray mode. This mode offers high deposition rate but due to tapering of electrode smaller diameter drops are formed. Continuous metal deposition, in form of drops, produces smooth bead and stiffer arc. Drawbacks of this metal transfer mode are: Minimum current for spray mode's being too high for some materials, large heat input to work piece, wide bead, and only down hand positional capability. In recent years, extensive research has been performed on pulsed current welding technique. GMAW-P is well known as a superior process to the conventional GMAW primarily due to its unique ability to introduce a significant influence on thermal characteristics of weld pool and rate of metal deposition at a given heat input by appropriate selection of pulse parameters [2].

GMAW-P is being increasingly used for joining wide variety of ferrous and non-ferrous materials in industries due to its inherent advantages, such as deep penetration, smooth weld bead, high welding speed, large metal deposition rate, lower spatter, lower distortion and lesser probability of porosity fusion defects. For GMAW-P, it is generally not easy and time consuming to establish usable working pulse condition by trial and error when adjusting pulse parameters. For achieving controlled transfer during pulse welding, it is essential that wire feed rate is balanced by burn rate. This means achieving one drop per pulse condition all the time, which involves constant control of all the pulse parameters. Synergic control is defined as any system by which pulse parameters (or wire feed speed) can be manipulated to achieve equilibrium over a wide range of wire feed speeds (or mean current levels). This mode of metal transfer overcomes the drawbacks of globular mode while achieving the benefits of spray transfer. This mode is characterized by pulsing of current between low-level background current and high-level peak current in such a way that mean current is always below the threshold level of spray transfer. The purpose of background current is to maintain arc where the peak currents are long enough to make sure detachment of the molten droplet [3-5].

A general premise to increase the fracture toughness of engineering steel is to ensure that the steel is characterized by fine-scale microstructure that is favorable and contains minimum harmful effects that can be induced by grain boundary precipitation or segregation of detrimental elements or inclusions, to name a few. Grain size reduction in weld zones confers the advantage of an improvement in mechanical properties. Because grain refinement has an advantage of markedly increasing strength as well as improving toughness of materials. It is therefore recommended that these steels are welded with a low heat input [6-9].

In this study, two welding processes, namely, GMAW and GMAW-P were employed in joining of AISI 1030 steel plates fabricated by ASP316L austenitic stainless steel filler metal.

2. Experimental procedure

10 mm thick of AISI 1030 steel couples were used as test materials. The chemical compositions and the mechanical properties of the welded material and welding wire are given in table 1 and 2. Welding was performed with a GMA mechanized unit (MIGATRONIC, KME 400 type), using a 1 mm diameter AISI 316L welding wire. The mixture of Ar + 2 % O_2 gas was used as shielding gas. Prior to welding, the plates were thoroughly cleaned to remove the oxide layer and any dirt or grease adherent to the V-groove (60^0 groove angle) surface. An arc voltage of 22.5 V, a welding speed of

TABLE 1
The chemical compositions and mechanical properties of the welded material (AISI 1030)

Chemical Composition (wt.%)							
Fe	**Cr**	**C**	**Ni**	**Si**	**Mo**	**S**	**Mn**
Bal.	–	0.267	–	0.177	–	0.053	1.13
Mechanical Properties							
Tensile Strength (N/mm^2)			**% Elongation (mm)**			**Hardness (HV)**	
485			25			82	

TABLE 2
The chemical compositions and mechanical properties of the welding wire (ASP316L)

Chemical Composition (wt.%)							
Fe	**Cr**	**C**	**Ni**	**Si**	**Mo**	**S**	**Mn**
Bal.	18	0.03	12	0.7	2.5	–	0.8
Mechanical Properties							
Tensile Strength (N/mm^2)			**% Elongation (mm)**			**Hardness (HV)**	
540-600			40			170	

Fig. 1. The general view of welded AISI 1030 steel couples

4 mm/s, a wire feeding speed of 3.2 m/min and a constant gas flow rate of 16 1/min were selected. The welding was carried out by filling the weld groove in multi-passes (2 passes) at the top and single pass at the bottom of each of them (Fig. 1).

After welding, cross-sectional samples were cut to analyze their microstructures and microhardness values. All welded samples were polished using a grit sequence of 200, 400, 600, 800, 1000 and 1200. These samples were further polished using cloth and polishing solution of 3 μm diamond paste. The samples of AISI 1030 were etched by chemical etching method with 2 % HNO_3+ 98 % pure alcohol in 2-3 s. The interface appearances of the etched samples were then examined by OM, SEM with attachment of EDS.

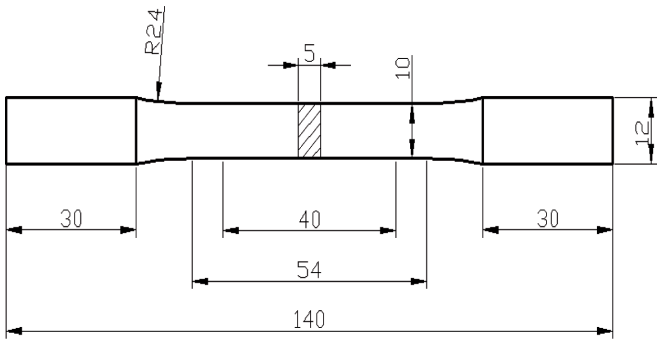

Fig. 2. Tensile test specimen

In this study, LEO, EVO 40XVP model Scanning Electron Microscopy was used. At the same time the breaking off surfaces of tensile specimens was examined by SEM. EDS analysis was done by BRUKER 125 eV type device to pick up the elementary contents of phases which were formed at the interface appearance of the welded samples. SHIMADZU XRD-6000 type X-ray analysis device was used to pick up the phases and compounds which occurred at the welded samples.

The mechanical properties of the weldments were evaluated by means of tensile, microhardness and impact tests. Standard tensile specimens were prepared according to the EN ISO 6892-1:2010 (Fig. 2). The specimens were removed from the materials in such a way that the weld was located in the center of each specimen and the samples were machined transverse to the welding direction. The tensile tests were carried on a HOUNSFIELD (50000 N) tensile test machine at a cross head speed of 2 mm/min. The microhardness of weld metal and the heat affected zones (HAZ) were measured with a Leica MHF-10 microhardness test machine at different points by Vickers microhardness method. A 200 g load was used in the measurement.

Impact test specimens were prepared in 50×10×10 dimensions for the mechanical examination. The impact tests were carried on a INSTRON WOLPERT PW30 (300 J) impact test machine.

3. Results and discussion

Figure 3,4 and 5,6 show optical micrographs and scanning electron microscope (SEM) images of intersections of welded S1 and S2 samples respectively. When the microstructures of S1 (GMAW) and S2 (GMAW-P) samples are analyzed, two different microstructures, which belong to stainless steel weld metal and carbon steel are seen. In the side of AISI 1030 of both samples, there are plenty of acicular ferrite islands in transition zone adjacent to weld metal. Acicular ferrities occurred mostly in melting boundary and free surface of the material where cooling rate is high [10]. In the coarse-grained zone, large number of Widmannstätten ferrite, grain boundary ferrite, plate and lath-type martansite, which are beginning from grain boundary are available. Moreover, the occurrence of grain-coarse is seen in the region where welded joints are adjacent to carbon steel melting boundary. In addition, it is seen that austenitic weld metal formed a regular and symmetrical connected region with both material and welding seam constituted of a very smooth welding. When Figure 3 and 4 compared with each other, the increase of grain-coarsing depending on the heat input increases in S1 sample was seen in the heat affected zone (HAZ). In a study, it has been reported that high energy input slow down cooling and solidification enough and caused more coarsing in the structures in this case of it [11]. The weld metal microstructure, which occurred as dendritic solidification in the weld seam, consists of austenite grains which are equal to each other and chromium carbide particles which scattered randomly around fine-grain interior and grain boundaries. The precipitation of these carbide particles allows of resistance of distribution, but it can also lead to fragility [12]. When S2 sample in Figure 7 is analyzed in terms of the EDS analysis, it is seen that while the diffusion carbon elements occurs from AISI 1030 to the weld metal, chromium diffusion from the weld metal to AISI 1030 in the same distance. The phase and compounds occurred in welded joint were analyzed by x-ray and austenite, $Cr_{23}C_6$, Cr_7C_3, Fe_3C phase and compounds were identified and given Figure 8.

When S1 and S2 welded joints are examined in terms of micro hardness analysis (Figure 9), the increase of the amount of hardness to the weld seam zone and then the decrease of the base material to hardness value are observed. The transition of carbon atoms, which were subjected to the diffusion towards weld metal by AISI 1030 steel, is thought as the reason of these events. In the center of weld metal, the highest hardness was obtained as HV340 for the S2 sample and HV311 for the S1 sample. The emergency of the high values of microhardness in the weld seam is due to the emergency of chromium-carbide phases which increases the hardness here. In addition, the ASP316L electrode which is used as the weld metal increased the hardness of the weldment. The reason of its due to the high rate of molybdenum element which exists in nature of weld electrode. Because, the aim of adding molybdenum to weld metal is increasing weld toughness and strength [13].

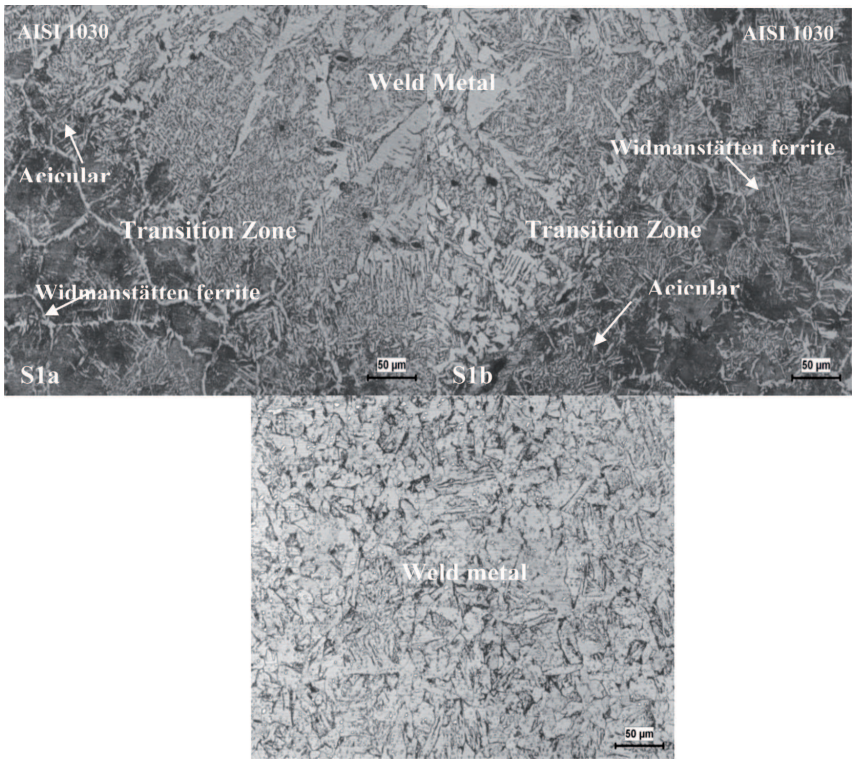

Fig. 3. Microstructure of the S1 sample a) Side of AISI 1030 and transition zone b) Side of AISI 1030 and transition zone

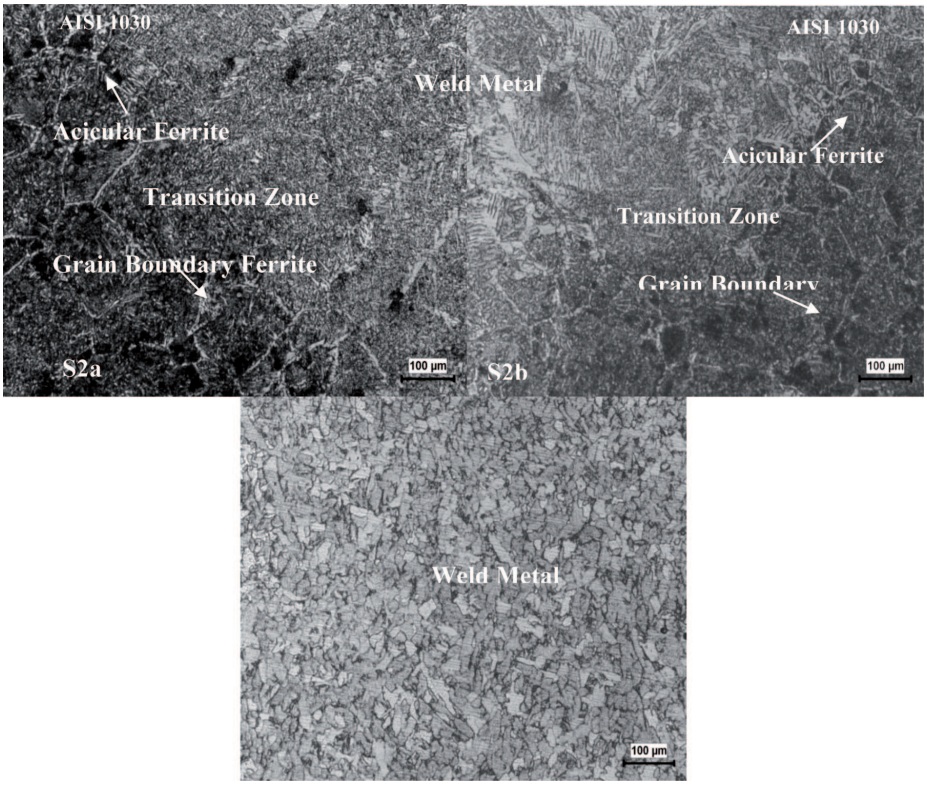

Fig. 4. Microstructure of the S2 sample S2a) Side of AISI 1030 and transition zone S2b) Side of AISI 1030 and transition zone

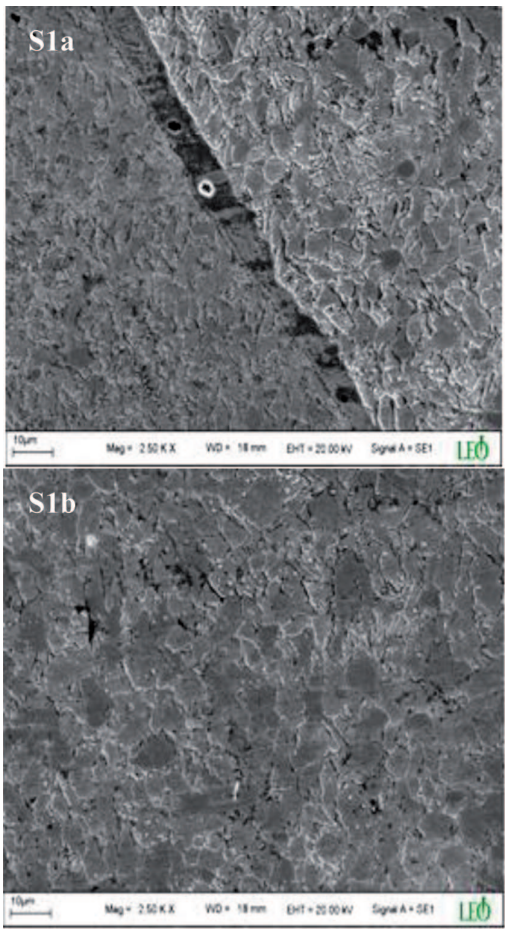

Fig. 5. SEM microstructure of the S1 sample a) Side of AISI 1030 b) Weld Metal

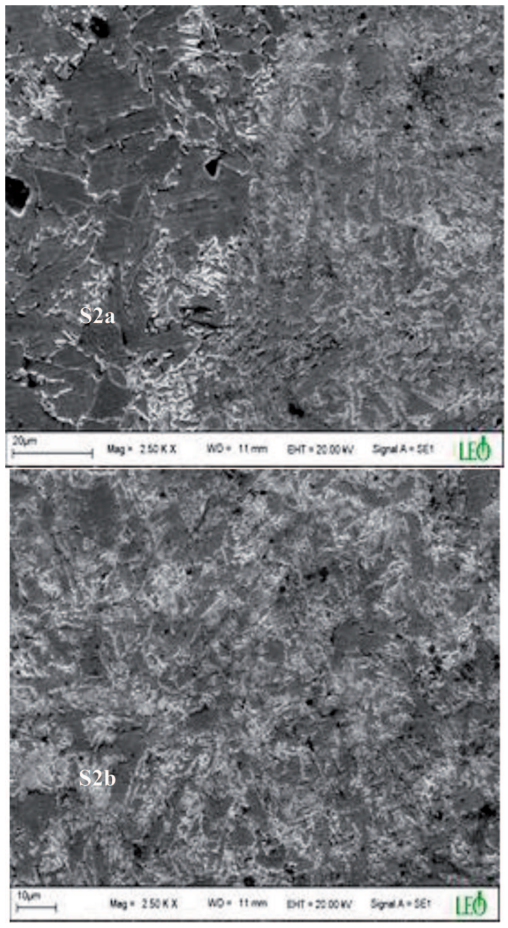

Fig. 6. SEM microstructure of the S2 sample a) Side of AISI 1030 b) Weld Metal

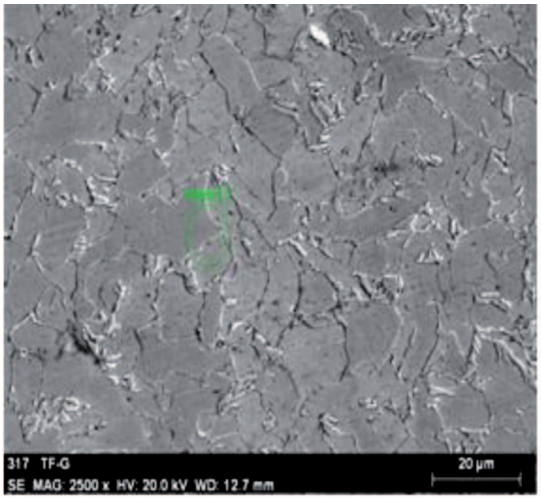

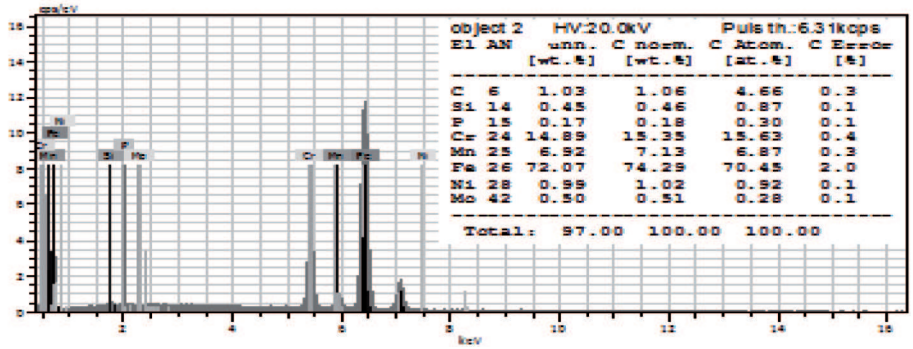

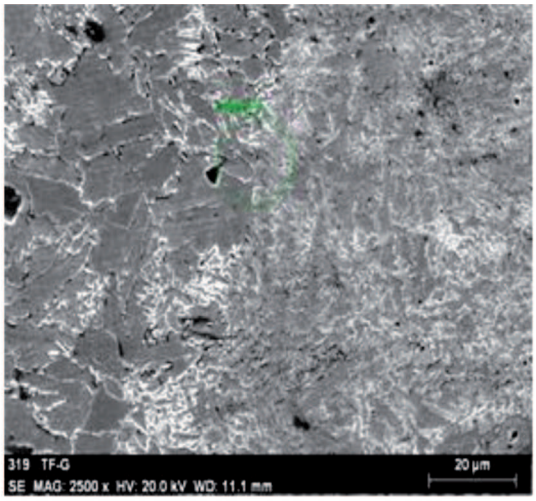

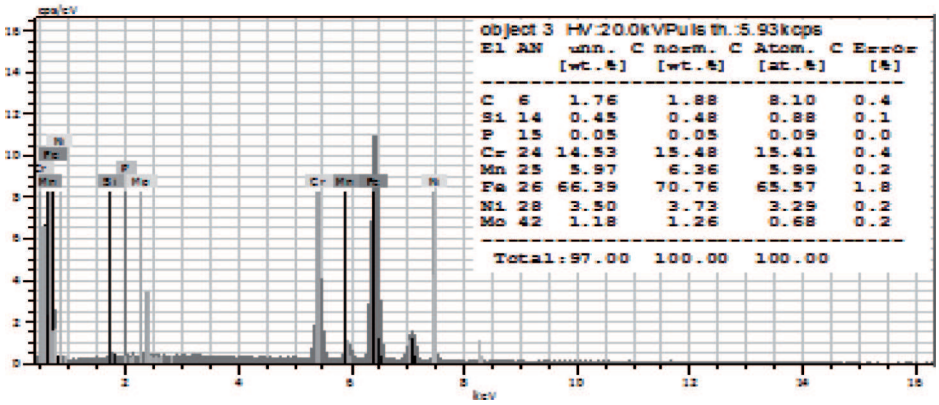

Fig. 7. EDS analysis of S2 sample

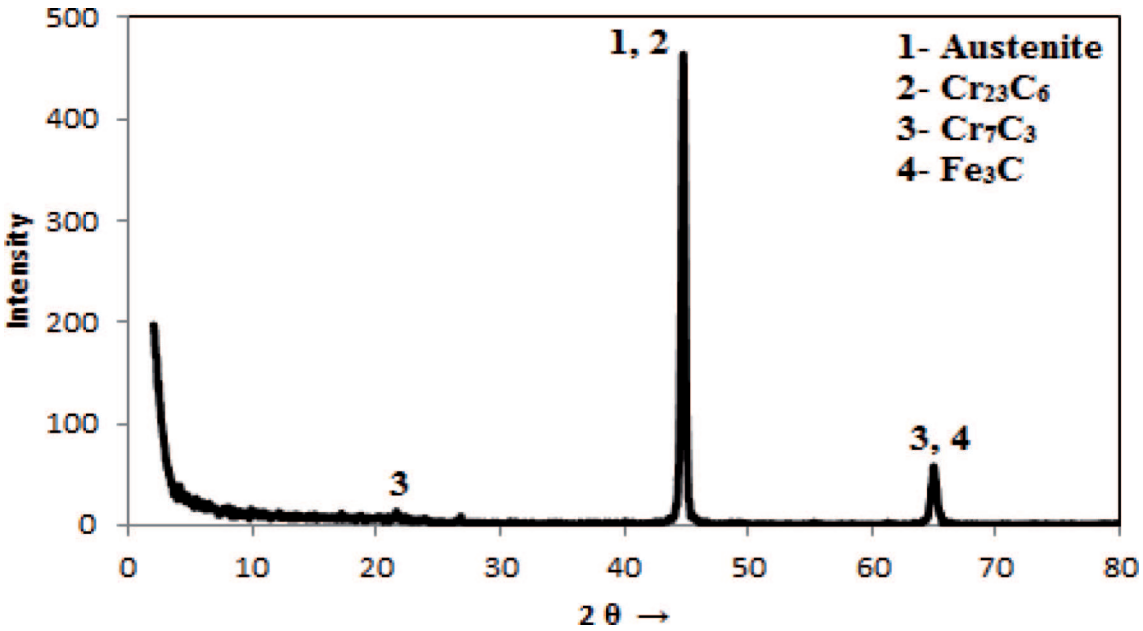

Fig. 8. XRD analysis of S2 sample

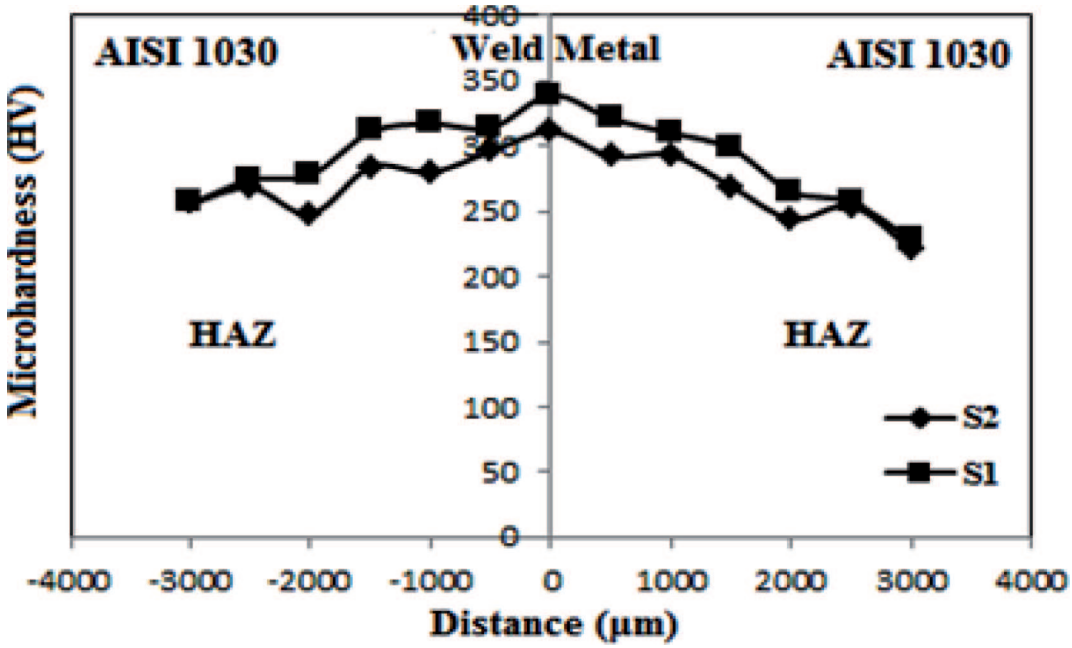

Fig. 9. Microhardness graphics of S1-S2 samples

The common feature here is in both welding the reduction in the hardness beginning from the line of transition zone. The blending of carbon steel and welding electrode with (Mo, Mn) elements which increase hardness in welding electrode is thought as the reason of it. In addition, the low heat input of joints which are obtained using GMAW-P and the grains occurring in weld metal due to the rapid solidification occurred as small and fine structure. Therefore the hardness values of weld metal which is obtained using GMAW-P has higher values than those obtained with GMAW [11].

As a result of tensile tests to determine the maximum strength values of test specimens, the maximum strength values 424.7 N/mm^2 for S1 sample and 459 N/mm^2 for S2 sample were obtained. In the % elongation values S1 sample, a significant decrease was recorded according to S2 sample. It is determined that the materials were broken by weld metal during the tensile test without showing adequate growth and making concession. In both samples, the emergence of fracture in the side of AISI 1030, after the welding process of carbon steel the rapid cooling –induced martensite tran-

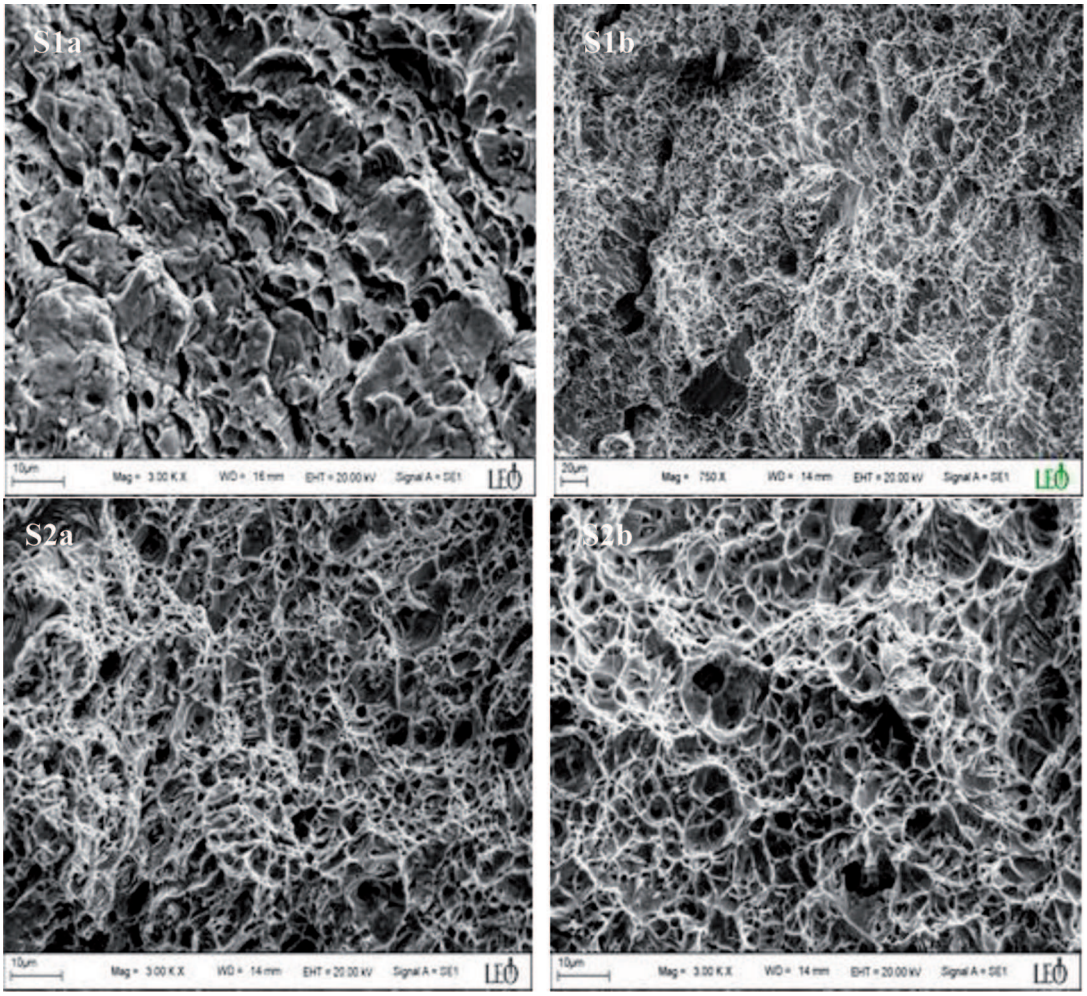

Fig. 10. Fracture surfaces of tensile tested specimens of S1 and S2 joints

sformation in the area adjacent to post-connected area and the decrease of toughness and ductility because of grain coarsening are known. Depending on the increasing weld improvement, the increase of tensile strength is observed, also. When the notch impact test results (obtained at room temperature) of AISI 1030 medium carbon steel plates combined with austenitic filler metal (ASP316L electrode) was examined, the highest impact energy were obtained 198 J for S2 sample and 199 J for S1 sample respectively. Recently, stainless steel electrodes (ASP316L electrode) are known to be resistant to hot cracking, because they are manufactured providing always some ferrite in the weld metal. The presence of a small amount of ferrite in the austenite structure increases the strength of welded joints [14]. Hawing greater toughness of S2 sample combined with the GMAW-P is due to fact that there are excessive grain coarsening in both sides depending on the more heat input in the sample S1.

Photos of fracture surface after tensile test specimens are shown in Figure 10. As can be seen in photographs in different sizes with uniform distribution and particles with hetergeneous distribution exhibit ductile fracture mechanism.

4. Conclusions

The following conclusions have been drawn concerning effect of the GMAW and the GMAW-P welding processes on microstructure, hardness, tensile and impact strength of AISI 1030 steel joints fabricated by ASP316L austenitic stainless steel filler metal:

1. Joining of 10 mm thick of AISI 1030 steel couples can be combined successfully with GMAW and GMAW-P techniques by using ASP316L austenitic stainless steel filler metal.
2. GMAW-P joints of AISI 1030 steel couples exhibit less grain growth when compared to GMAW joints in HAZ.
3. The highest impact strength value was measured in the S2 sample which is performed with GMAW-P technique. The grain growth because of the high heat

input occurring in GMAW technique causes the decrease of impact strength values in the joint.

4. The highest hardness value in the center of weld metal in S2 sample which is performed with GMAW-P technique. The low heat input in GMAW-P and the fine grains occurring in the weld metal due to the rapid solidification and shaped as small and slender-structured, increased the hardness value.

REFERENCES

[1] W.R. Oates, A.M. Saitta, Weldind handbook, materials and applications-part 2, Volume 4, American Welding Society (1998).

[2] K. Devakumaran, P.K. Ghosh, Thermal characteristics of weld and HAZ during pulse current gas metal arc weld bead deposition on HSLA steel plate, Materials and Manufacturing Processes **25**, 616-630 (2010).

[3] P. Praveen, PKDV. Yarlagadda, Meeting challenges in welding of aluminum alloys through pulse gas metal arc welding, Journal of Materials Processing Technology **164-165**, 1106-1112 (2005).

[4] P. Sukhomay, K.P. Suriya, K.S. Arun, Determination of optimal pulse metal inert gas welding parameters with a neuron-GA technique, Materials and Manufacturing Processes **25**, 606-615 (2010).

[5] M. Balasubramanian, V. Jayabalan, V. Balasubramanian, Optimizing the pulsed current GTAW parameters to attain maximum impact toughness, Materials and Manufacturing Processes **23**, 69-73 (2008).

[6] R. Manti, D.K. Dwivedi, Microstructure of Al-Mg-Si weld joints produced by pulse TIG welding, Materials and Manufacturing Processes **22**, 57-61 (2007).

[7] E. Taban, A. Dhooge, E. Kaluç, Plasma arc welding of modified 12% Cr stainless Steel, Materials and Manufacturing Processes **24**, 649-656 (2009).

[8] R.D.K. Misra, Understanding strength-toughness combination in the processing of engineering steels, Materials and Manufacturing Processes **25**, 60-71 (2010).

[9] L. Du, S. Yao, M. Xiong, X. Liu, G. Wang, Austenite grain ultrarefinement and the formation of nanocrystallized structure through transformation of low carbon steels, Materials and Manufacturing Processes **25**, 26-32 (2010).

[10] S. Kou, Welding metallurgy 2. edition, John Wile & Sons, (2003).

[11] M.V. Suresh, B.V. Krishna, P. Venugopal, K.P. Rao, Effect of pulse frequency in gas tungsten arc welding of powder metallurgical preforms, Science And Technology of Welding & Joinning **9**, 362-368 (2004).

[12] M. Erdoan, Malzeme bilimi ve mühendislik malzemeleri, Nobel Yayın Dağıtım **1**, 326-332 (2002).

[13] K. Tülbentçi, Mig-Mag Gazaltı Kaynak Yöntemi, Arctech Yayını, (1998).

[14] F. Kölük, Östenitik paslanmaz çeliklerin kaynağında kaynak yönteminin ısı tesiri altında kalan bölgeye etkisinin incelenmesi, G.Ü.F.B.E., Yüksek Lisans Tezi, (2000).

Received: 15 April 2011.